New functional form to describe the temperature dependence of liquid phase reaction rates

Yunsie Chung[a], William H. Green[a,*]

[a]*Department of Chemical Engineering, Massachusetts Institute of Technology, Cambridge, MA, U.S.A*

ABSTRACT

Chemical reactions in subcritical or near-critical solvents hold significant promise for numerous industrial and environmental applications. The Arrhenius equation is typically used to describe the temperature dependence of reaction rates, yet it often falls short in capturing the behavior of liquid phase reaction rates near critical points of solvents. To address this limitation, we propose a novel functional form that can correctly describe the temperature trends of liquid phase rate constants from room temperature up to the critical temperature of a solvent. The proposed scheme uses four kinetic parameters with physical implications, two accounting for the gas phase contribution and the other two accounting for the solvation effect on reactions. The new functional form can accurately reproduce the anomalous temperature dependence of liquid phase rate constants in subcritical and near-critical regimes that the Arrhenius equation fails to capture. Furthermore, our preliminary finding suggests that the kinetic parameters associated with the solvation terms can be computed with ab initio approaches to estimate the temperature-dependent rate constants of liquid phase reactions based on their corresponding rate constants in gas phase. The proposed functional form provides an alternative approach to describe the non-Arrhenius behavior of diverse liquid phase reactions across a wide range of temperature.

1. Introduction

Chemical reactions in subcritical or near-critical solvents have been the subject of great interest in many industrial and environmental applications [1, 2, 3, 4]. Kinetic rates and selectivity of various industrially relevant reactions, such as dehydration of alcohols, Diels-Alder, alkylation, and cyclization, can be enhanced in subcritical water or organic solvents [1, 5, 6, 7]. Waste plastics can be effectively decomposed and recycled by depolymerization reactions in subcritical water or alcohols [8, 9, 10, 11]. Subcritical fluids also serve as excellent reaction media for the conversion of biomass to fuels and other valuable chemicals [12, 13, 14]. In nuclear power plants, subcritical or supercritical water is used as a coolant for a reactor, and a knowledge of the kinetic mechanisms of water radiolysis is essential for designing a safe water-coolant reactor that can suppress the formation of oxidizing species and mitigate corrosion [15, 16, 17, 18].

Due to the high interest in the chemistry of subcritical systems, kinetic rates of many liquid phase reactions have been measured and investigated under subcritical conditions. They are typically measured at multiple temperatures under constant pressure and fitted to the Arrhenius equation, which can then be used to estimate rate constants at different temperatures. The Arrhenius equation [19] is the most widely used functional form for describing the temperature (T) dependence of a rate constant (k) and has a following form:

$$k = A \exp\left(\frac{-E_a}{RT}\right) \tag{1}$$

where A is the pre-exponential factor, E_a is the activation energy, and R is the universal gas constant. The Arrhenius equation assumes a linear relationship between $\ln k$ and $1/T$ and treats A and E_a as temperature-independent

*Corresponding author

✉ whgreen@mit.edu (W.H. Green)
ORCID(s): 0000-0002-3097-010X (Y. Chung); 0000-0003-2603-9694 (W.H. Green)

parameters. While most reactions show the linear dependence, many liquid phase reactions start to exhibit non-Arrhenius behavior as temperature approaches a critical point of a solvent [15, 16, 20, 21, 22, 18]. Near a critical point, the physicochemical properties of a solvent change dramatically with a slight variation of temperature, and as a result, rapid slowing-down or acceleration of rate constants are observed for many liquid phase reactions at elevated temperatures. A modified version of the Arrhenius equation is frequently used to describe more complex temperature dependence of a rate constant:

$$k = AT^n \exp\left(\frac{-E_a}{RT}\right) \tag{2}$$

where n is introduced as an additional empirical parameter. The modified equation can cover a wider temperature range than the conventional Arrhenius equation, but it still fails to capture the anomalous temperature dependence of liquid phase reactions in subcritical regions.

In an alternative approach, the temperature dependence of a liquid phase rate constant (k_{liq}) is explained in terms of gas phase and solvation contributions [23, 24, 25, 16, 26]:

$$k_{\text{liq}} = A \exp\left(-\frac{E_a + \Delta\Delta G^{\ddagger}_{\text{solv}}}{RT}\right) \tag{3}$$

where $\Delta\Delta G^{\ddagger}_{\text{solv}}$ represents the solvation effect on the free energy of activation, and A and E_a are the gas phase kinetic parameters of the same reaction. The $\Delta\Delta G^{\ddagger}_{\text{solv}}$ term accounts for the difference between the solvation free energies of the reactants and transition state (TS). This approach assumes A and E_a to be constant and attempts to describe the non-Arrhenius behavior of k_{liq} in terms of the temperature dependence of $\Delta\Delta G^{\ddagger}_{\text{solv}}$. As temperature approaches the critical point of a solvent, the solvent's dielectric constant changes significantly, causing the $\Delta\Delta G^{\ddagger}_{\text{solv}}$ value to change a lot for the reaction whose reactants and TS have different dipole moments. Marrone, Tester, and their co-workers [23, 24] adopted the Kirkwood theory [27] to express $\Delta\Delta G^{\ddagger}_{\text{solv}}$ as a function of the dielectric constant of a solvent and the dipole moments and molecular radii of reactants and TS. While they were able to reproduce the experimental data of CH_2Cl_2 hydrolysis from room temperature up to the critical point of water, their method relies on several variables that cannot be easily fitted to experimental data.

An alternative functional form that can describe the temperature dependence of k_{liq} with minimal empirical parameters is needed. Previously, we have developed a correlation to predict the solvation free energy of a species from around 250 K up to the critical temperature of a solvent with only two solvation properties [28]. The correlation was able to provide accurate predictions for a variety of solvent-solute pairs only based on the solvation free energy and solvation enthalpy at 298 K and the solvent's density. In this work, we apply the same correlation to estimate the solvation free energies of the reactants and TS of a reaction, hence estimating the $\Delta\Delta G^{\ddagger}_{\text{solv}}$ across a range of temperatures. Our proposed method only needs two parameters to express the temperature dependence of $\Delta\Delta G^{\ddagger}_{\text{solv}}$, which can be easily fitted to experimental data or potentially calculated using ab initio methods. The devised method can be combined with the Arrhenius equation to accurately reproduce the experimental rate constants of diverse liquid phase reactions for a wide range of temperature.

2. Method

2.1. Derivation of the new functional form

The overview of our approach is illustrated in Figure 1. Our method uses the previously developed correlation [28] to approximate the temperature dependence of $\Delta\Delta G^{\ddagger}_{\text{solv}}$ and subsequently employs eq 3 to express the liquid phase rate constant as a function of Arrhenius parameters and $\Delta\Delta G^{\ddagger}_{\text{solv}}$. Eq 3 is derived based on the assumption that the same reaction occurs in both gas and liquid phases [25], which allows the liquid phase rate constant to be expressed in terms
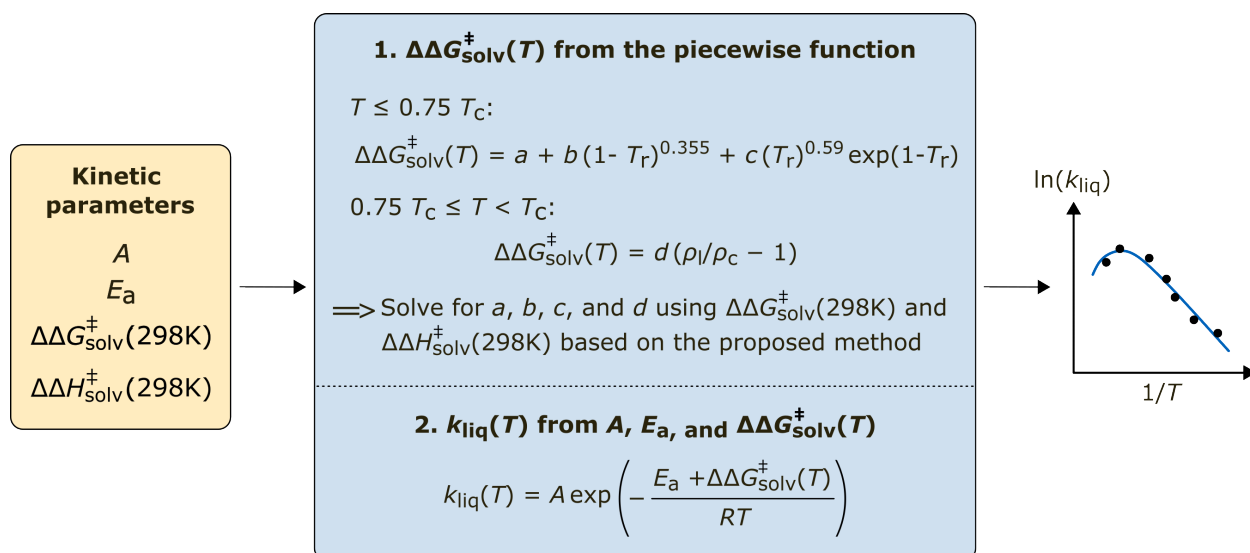
Figure 1: Overview of the method for estimating the temperature dependence of a liquid phase rate constant.

of the corresponding gas phase rate constant (k_{gas}) and solvation correction [25]:

$$k_{\text{liq}} = k_{\text{gas}} \exp\left(\frac{-\Delta\Delta G^{\ddagger}_{\text{solv}}}{RT}\right) = A \exp\left(-\frac{E_a + \Delta\Delta G^{\ddagger}_{\text{solv}}}{RT}\right) \tag{4}$$

In eq 4, it is also assumed that k_{gas} follows the Arrhenius form ($k_{\text{gas}} = A \exp\left(\frac{-E_a}{RT}\right)$) and the transmission coefficient for quantum tunneling effects is similar between gas phase and liquid phase. The solvation correction term, $\Delta\Delta G^{\ddagger}_{\text{solv}}$, is defined as the difference between the solvation free energy of the TS ($\Delta G^{\text{TS}}_{\text{solv}}$) and the solvation free energy of the reactant ($\Delta G^{\text{R}}_{\text{solv}}$):

$$\Delta\Delta G^{\ddagger}_{\text{solv}} = \Delta G^{\text{TS}}_{\text{solv}} - \Delta G^{\text{R}_i}_{\text{solv}} \tag{5}$$

Solvation free energy (ΔG_{solv}) is a change in Gibbs free energy associated with the transfer of a solute molecule from a gas phase to a solution phase. In our earlier work [28], we combined two existing correlations [29, 30], which were developed based on thermodynamic relationships, and formulated a piecewise function that can predict the solvation free energy of a solvent-solute pair for a broad range of temperature:

For $T \leq 0.75 T_c$:

$$\Delta G_{\text{solv}}(T) = a + b(1 - T_r)^{0.355} + c(T_r)^{0.59} \exp(1 - T_r) + RT \ln\left(\frac{\rho_g(T)}{\rho_l(T)}\right) \tag{6}$$

For $0.75 T_c \leq T < T_c$:

$$\Delta G_{\text{solv}}(T) = d\left(\frac{\rho_l(T)}{\rho_c} - 1\right) + RT \ln\left(\frac{\rho_g(T)}{\rho_l(T)}\right) \tag{7}$$

where T_c is the solvent's critical temperature, T_r is the reduced temperature ($T_r = \frac{T}{T_c}$), ρ_c is the solvent's critical density, and $\rho_g(T)$ and $\rho_l(T)$ are the solvent's gas-phase and liquid-phase saturation densities at temperature T, respectively.

The lower case letters, a, b, c, and d, represent the empirical parameters that are unique to each solvent-solute pair. We have previously demonstrated that the piecewise function (eq 6 and 7) can provide accurate ΔG_{solv} predictions up to the critical temperature of a solvent for various closed-shell compounds in solution [28].

In this work, we assume that the piecewise function is applicable to any compounds, transition states, and particles dissolved in a solvent. We plug eq 6 and 7 into eq 5 to get the following relationships:

For $T \leq 0.75T_{\text{c}}$:

$$\Delta\Delta G_{\text{solv}}^{\ddagger}(T) = (a^{\text{TS}} - a^{\text{R}}) + (b^{\text{TS}} - b^{\text{R}})(1 - T_{\text{r}})^{0.355} + (c^{\text{TS}} - c^{\text{R}})(T_{\text{r}})^{0.59} \exp\left(1 - T_{\text{r}}\right) \quad (8)$$

For $0.75T_{\text{c}} \leq T < T_{\text{c}}$:

$$\Delta\Delta G_{\text{solv}}^{\ddagger}(T) = (d^{\text{TS}} - d^{\text{R}})\left(\frac{\rho_{\text{l}}(T)}{\rho_{\text{c}}} - 1\right) \quad (9)$$

where a^{TS}, b^{TS}, c^{TS}, and d^{TS} represent the empirical parameters of the TS and a^{R}, b^{R}, c^{R}, and d^{R} represent the empirical parameters of the reactant. The equations can be simplified by lumping the two empirical parameters as follow:

For $T \leq 0.75T_{\text{c}}$:

$$\Delta\Delta G_{\text{solv}}^{\ddagger}(T) = a + b(1 - T_{\text{r}})^{0.355} + c(T_{\text{r}})^{0.59} \exp\left(1 - T_{\text{r}}\right) \quad (10)$$

For $0.75T_{\text{c}} \leq T < T_{\text{c}}$:

$$\Delta\Delta G_{\text{solv}}^{\ddagger}(T) = d\left(\frac{\rho_{\text{l}}(T)}{\rho_{\text{c}}} - 1\right) \quad (11)$$

where a, b, c, and d now represent the empirical parameters unique to each reaction-solvent pair. Eq 11 ensures that $\Delta\Delta G_{\text{solv}}^{\ddagger}$ approaches a correct limit of zero as temperature approaches a critical point. More details on the critical limit can be found in the dedicated work of Japas and Levelt Sengers [30] and in our prior study [28].

In order to solve for the four empirical parameters (a, b, c, d), four equations are needed. We use the same approach as our earlier work [28] and obtain two equations by forcing the piecewise function shown in eq 10 and 11 to match in value and gradient at the transition temperature:

At $T = 0.75T_{\text{c}}$:

$$a + b(1 - T_{\text{r}})^{0.355} + c(T_{\text{r}})^{0.59} \exp\left(1 - T_{\text{r}}\right) = d\left(\frac{\rho_{\text{l}}(T)}{\rho_{\text{c}}} - 1\right) \quad (12)$$

$$-\frac{0.355b}{T_{\text{c}}}(1 - T_{\text{r}})^{-0.645} + \frac{c \exp\left(1 - T_{\text{r}}\right)}{T_{\text{c}}}\left(0.59(T_{\text{r}})^{-0.41} - (T_{\text{r}})^{0.59}\right) = \frac{d}{\rho_{\text{c}}}\frac{\text{d}\rho_{\text{l}}}{\text{d}T} \quad (13)$$

The $\Delta\Delta G_{\text{solv}}^{\ddagger}$ values or its gradients (enthalpy or entropy) at two temperatures are needed to obtain two additional equations. Our two prior studies [31, 32] demonstrated that the ab initio COSMO-RS method can provide reasonable estimations of $\Delta\Delta G_{\text{solv}}^{\ddagger}$ and $\Delta\Delta H_{\text{solv}}^{\ddagger}$ at 298 K for various liquid phase reactions. Thus, we formulate two more equations based on the $\Delta\Delta G_{\text{solv}}^{\ddagger}$ and $\Delta\Delta H_{\text{solv}}^{\ddagger}$ values at 298 K:

At $T = 298$ K :

$$a + b(1 - T_r)^{0.355} + c(T_r)^{0.59} \exp(1 - T_r) = \Delta\Delta G_{solv}^{\ddagger}(298 \text{ K}) \tag{14}$$

$$-\frac{0.355b}{T_c}(1 - T_r)^{-0.645} + \frac{c\exp(1 - T_r)}{T_c}\left(0.59(T_r)^{-0.41} - (T_r)^{0.59}\right)$$
$$= -\frac{\Delta\Delta H_{solv}^{\ddagger}(298 \text{ K}) - \Delta\Delta G_{solv}^{\ddagger}(298 \text{ K})}{298 \text{ K}} \tag{15}$$

where the right-hand side of eq 15 is equivalent to the temperature gradient of $\Delta\Delta G_{solv}^{\ddagger}$ at 298 K:

$$\frac{d\Delta\Delta G_{solv}^{\ddagger}}{dT}\bigg|_{T=298 \text{ K}} = -\Delta\Delta S_{solv}^{\ddagger}(298 \text{ K}) = -\frac{\Delta\Delta H_{solv}^{\ddagger}(298 \text{ K}) - \Delta\Delta G_{solv}^{\ddagger}(298 \text{ K})}{298 \text{ K}} \tag{16}$$

With a set of four equations (eq 12 - 15) that are linear with respect to a, b, c, and d, we can solve for those four parameters based on $\Delta\Delta G_{solv}^{\ddagger}(298 \text{ K})$, $\Delta\Delta H_{solv}^{\ddagger}(298 \text{ K})$, and the saturation densities ($\rho_l(T)$) and critical properties (T_c, ρ_c) of a solvent. The densities and properties of many common solvents can be obtained using open-source models, such as fluid thermodynamics packages CoolProp [33] and Clapeyron.jl [34], and a machine learning model developed by Biswas et al.[35] Since the solvent's properties are easily obtainable from the existing models, we can treat them as known values. Thus, only $\Delta\Delta G_{solv}^{\ddagger}(298 \text{ K})$ and $\Delta\Delta H_{solv}^{\ddagger}(298 \text{ K})$ are needed to solve for the four empirical parameters and hence obtain $\Delta\Delta G_{solv}^{\ddagger}$ at any temperature. The computed $\Delta\Delta G_{solv}^{\ddagger}(T)$ values can be subsequently combined with the gas phase kinetic parameters (A, E_a) as shown in 4 to obtain a liquid phase rate constant.

In summary, our proposed approach allows us to describe the temperature dependence of a liquid phase rate constant in terms of four kinetic parameters: (1) A, (2) E_a, (3) $\Delta\Delta G_{solv}^{\ddagger}(298 \text{ K})$, and (4) $\Delta\Delta H_{solv}^{\ddagger}(298 \text{ K})$. Here, A and E_a account for the Arrhenius behavior while $\Delta\Delta G_{solv}^{\ddagger}(298 \text{ K})$ and $\Delta\Delta H_{solv}^{\ddagger}(298 \text{ K})$ account for the solvation effect that exhibits non-Arrhenius behavior.

The method developed in our earlier study [28] estimates the temperature-dependent solvation free energy at a solvent's saturation pressure, and thus $\Delta\Delta G_{solv}^{\ddagger}$ is also estimated along a solvent's saturation curve. This indicates that the gas phase rate constant (k_{gas}) in eq 4 should correspond to the values at the saturation pressure for pressure-dependent reactions. Yet, our earlier work [28] demonstrated that the method can provide reasonable predictions of solvation free energy at higher pressures as well as long as the temperature is not too close to the critical temperature of the solvent ($T < 0.8T_c$). Near a critical point, the pressure effect becomes more significant, and therefore our method is expected to have a higher error if the pressure deviates from the saturation pressure at elevated temperatures ($0.8T_c < T$). Moreover, our method assumes the dilute limit, which may not be valid if a substantial amount of a reactant is dissolved or if the solvent is a reactant.

2.2. Method validation: fitting the four kinetic parameters

The proposed method is tested by fitting the four kinetic parameters (A, E_a, $\Delta\Delta G_{solv}^{\ddagger}(298 \text{ K})$, $\Delta\Delta H_{solv}^{\ddagger}(298 \text{ K})$) to the experimental data of liquid phase rate constants and calculating the rate constants with the fitted parameters. For each reaction, the four kinetic parameters are optimized by minimizing the following loss function:

$$L = \sqrt{\frac{\sum_{i=1}^{N}\left(\log_{10}(k_{liq,expt}) - \log_{10}(k_{liq,calc})\right)^2}{N}} + \lambda\left((\Delta\Delta G_{solv}^{\ddagger}(298 \text{ K}))^2 + (\Delta\Delta H_{solv}^{\ddagger}(298 \text{ K}))^2\right) \tag{17}$$

$$k_{liq,calc} = f\left(A, E_a, \Delta\Delta G_{solv}^{\ddagger}(298 \text{ K}), \Delta\Delta H_{solv}^{\ddagger}(298 \text{ K})\right)$$

where λ is a regularization term, $k_{liq,expt}$ is an experimental rate constant, and $k_{liq,calc}$ is a calculated rate constant which is a function of the kinetic parameters to be optimized. The regularization term is added in eq 17 to prevent the solvation parameters ($\Delta\Delta G_{solv}^{\ddagger}(298 \text{ K})$, $\Delta\Delta H_{solv}^{\ddagger}(298 \text{ K})$) from being overfitted to the experimental data. The optimal

value of λ is identified as 0.0001 when a kcal/mol unit is used for the solvation parameters in the loss function. Only the solvation parameters are regularized as their values typically fall within ± 7 kcal/mol for most reactions and larger values are rare unless the polarity of the TS is significantly different from that of the reactants [32]. We also found that adding the regularization term for the solvation parameters provides more reasonable results for the optimized kinetic parameters.

The initial guesses of $\Delta\Delta G^{\ddagger}_{\text{solv}}$(298 K) and $\Delta\Delta H^{\ddagger}_{\text{solv}}$(298 K) are arbitrarily set to -1 kcal/mol and -1.5 kcal/mol, respectively, while the initial guesses of the Arrhenius parameters, A and E_a, are determined based on the experimental data. To find the best initial guesses for A and E_a, the $\ln k$ vs $1/T$ plot is first made using the experimental data, and a linear line is fitted only using the data points at a lower temperature region (around $T < 0.75T_c$) where the Arrhenius behavior is observed. Then the fitted linear line is vertically shifted to match the experimental $\ln k$ values near T_c. Finally, the initial guesses of A and E_a are made based on the y-intercept (y-intercept = $\ln A$) and slope (slope = $-\frac{E_a}{R}$) of the resulting linear line. The vertical shifting step is necessary when generating the linear line because as temperature approaches T_c, $\Delta\Delta G^{\ddagger}_{\text{solv}}$ approaches zero (see eq 11) and k_{liq} consequently approaches $A \exp\left(\frac{-E_a}{RT_c}\right)$ (see eq 4). By ensuring that the linear line passes through the experimental $\ln k$ values near T_c, we can generate good initial guesses that lead to a correct critical limit.

The parameters are optimized with a constrained optimization function from the SciPy package [36]. The bounds of $\Delta\Delta G^{\ddagger}_{\text{solv}}$(298 K) and $\Delta\Delta H^{\ddagger}_{\text{solv}}$(298 K) are empirically set to $(-6\,\text{kcal/mol}, 4\,\text{kcal/mol})$ and $(-10\,\text{kcal/mol}, 8\,\text{kcal/mol})$, respectively. For A and E_a, two different sets of bounds are used to obtain two sets of optimized parameters, and the best set that gives the lowest residual error is selected as the final optimized values. The two sets of bounds used for A are $(\log_{10} A_{\text{init}} - 1, \log_{10} A_{\text{init}} + 1)$ and $(\log_{10} A_{\text{init}} - 2, \log_{10} A_{\text{init}} + 2)$ where A_{init} is the initial guess determined from the steps described previously. The bounds used for E_a are $(-\frac{E_{a,\text{init}}}{1000R} - 12, -\frac{E_{a,\text{init}}}{1000R} + 12)$ and $(-\frac{E_{a,\text{init}}}{1000R} - 12, 0)$ where $E_{a,\text{init}}$ is the initial guess. Finally, k_{liq} are calculated based on the optimized kinetic parameters and compared with the experimental data.

2.3. Method validation: calculating the solvation kinetic parameters

We additionally calculate k_{liq} using experimental k_{gas} data and the solvation parameters computed from ab initio methods to test whether our proposed method can yield accurate predictions without using any experimental k_{liq} data. The solvation parameters, $\Delta\Delta G^{\ddagger}_{\text{solv}}$(298 K) and $\Delta\Delta H^{\ddagger}_{\text{solv}}$(298 K), are calculated based on the computational approach described in Ref. 31; the geometries of reactants and TS are optimized at the ωB97XD/def2-TZVP level of theory [37, 38] using Gaussian16 [39], followed by the single-point COSMO-RS [40, 41, 42] calculations at the BP-TZVPD-FINE level [43, 44, 45, 46]. The COSMO-RS calculations are performed using TURBOMOLE 7.5 [47, 48] and COSMOtherm (release 2021) [49]. Temperature-dependent $\Delta\Delta G^{\ddagger}_{\text{solv}}$ values are then calculated using the computed $\Delta\Delta G^{\ddagger}_{\text{solv}}$(298 K) and $\Delta\Delta H^{\ddagger}_{\text{solv}}$(298 K) and combined with experimental k_{gas} data to obtain k_{liq} using eq 4.

3. Experimental data

Experimental data of liquid phase rate constants are collected from literature to evaluate the method. The data collection is limited to the reactions that have experimental rate constants across a wide range of temperature and exhibit non-Arrhenius behavior at elevated temperature. A total of 14 reactions that occur in water are collected as listed in Table 1. Due to the scarcity of experimental data, we were unable to find the reaction data for solvents other than water.

As Table 1 indicates, many of these reactions are fast bimolecular reactions that are affected by diffusion rates. Bimolecular liquid phase reactions with rate constants greater than around 3×10^9 M^{-1}s^{-1} at 298 K are usually influenced by diffusion limitations [15]. While diffusion effects diminish as temperature increases, it can affect the reaction rates up to around 473 K for fast reactions. For diffusion-controlled reactions, experimentally measured or observed rate constants do not correspond to their intrinsic rate constants but are the function of both diffusion and intrinsic rate constants. Observed rate constants (k_{obs}) of bimolecular reactions can be estimated as:

$$k_{\text{obs}} = \left(\frac{1}{k_{\text{diff}}} + \frac{1}{k_{\text{liq}}} \right)^{-1} \tag{18}$$

Table 1
List of experimental data collected from literature. All reactions occur in water.

Index	Reaction	Influenced by diffusion limit?	Ref
1	$\cdot OH + \cdot OH \longrightarrow H_2O_2$	Yes (both k_{liq} and k_{obs} reported)	15, 50
2	$H\cdot + O_2 \longrightarrow HO_2\cdot$	Yes (both k_{liq} and k_{obs} reported)	15, 21
3	$e^- + H^+ \longrightarrow H\cdot$	Yes	51, 52
4	$\cdot OH + C_6H_5NO_2 \longrightarrow \cdot OHC_6H_5NO_2$	Yes	53, 54, 55, 56
5	$\cdot OH + H_2 \longrightarrow H_2O + H\cdot$	No	16, 57
6	$OH^- + H\cdot \longrightarrow e^- + H_2O$	No	58, 59
7	$e^- + N_2O \longrightarrow N_2O^-$	No	60
8	$H\cdot + HO_2\cdot \longrightarrow H_2O_2$	Yes	21
9	$C_6H_5OH + \cdot OH \longrightarrow \cdot C_6H_5(OH)_2$	Yes	20
10	$C_6H_5OH + H\cdot \longrightarrow \cdot C_6H_6OH$	Yes	20
11	$\cdot C_6H_5(OH)_2 \longrightarrow C_6H_5O\cdot + H_2O$	No	20
12	$\cdot C_6H_5(OH)_2 \longrightarrow C_6H_5OH + \cdot OH$	No	20
13	$I_2^- + I_2^- \longrightarrow I_3^- + I^-$	Yes	22
14	$Mu + C_6H_6 \longrightarrow MuC_6H_6$	Yes	17

where k_{diff} is the diffusion rate constant and k_{liq} is the intrinsic liquid phase rate constant.

The original data sources [15, 50, 21] of Reactions 1 and 2 reported the estimated k_{liq} along with the k_{obs}. However, the majority of the studies only reported the k_{obs}, which are assumed to be diffusion-controlled to a certain extent. Since the true k_{liq} could not be determined for those reactions, we fitted our functional form to the experimental k_{obs} data for the fitting method described in Section 2.2. We did not separately account for the diffusion effects in our method as it is challenging to make accurate estimations of k_{diff} for the reactions investigated in this study and diffusion effects become negligible near a critical temperature of a solvent. It is shown that our method can still accurately reproduce the experimental rate constants of the diffusion-limited reactions as further discussed in the results section.

4. Results and discussion

4.1. Fitting the functional form

The results of the proposed functional form that are fitted to the experimental data are shown in Figure 2 as blue solid lines ($k_{\text{liq, fitted}}$) for individual reactions. The results of the fitted Arrhenius equation ($k_{\text{Arrhenius, fitted}}$, orange dashed line) are also provided in the figure for comparison. The experimental data of intrinsic rate constants ($k_{\text{liq, expt}}$) and observed rate constants ($k_{\text{obs, expt}}$) are represented in circular markers and diamond markers, respectively.

Figure 2 shows that our functional form outperforms the Arrhenius equation for all reactions. Our method can accurately reproduce the experimental rate constants for the entire temperature range up to the critical temperature of the solvent while the Arrhenius equation starts to deviate from the experimental data above around 400 K. The mean absolute error (MAE) and root-mean-square error (RMSE) of each method are summarized in Table 2. Three different errors are computed by using (1) the entire range of temperature (All T), (2) temperature below 400 K ($T \leq 400$ K), and (3) temperature above 400 K (400 K $< T$). It can be seen that our fitted functional form has a much lower error with a MAE/RMSE of 0.07/0.09 in $\log_{10} k_{\text{liq}}$ for the entire T range compared to the Arrhenius equation that has a MAE/RMSE of 0.25/0.35 in $\log_{10} k_{\text{liq}}$. Below 400 K, both the proposed functional form and the Arrhenius equation have similar fitting errors. However, at elevated temperatures above 400 K, the Arrhenius form cannot fit to the experimental data well and has a substantially higher error. Our proposed functional form, on the contrary, has a consistently low error for all temperature ranges.

From Figure 2, it can be seen that the reactions mostly exhibit the Arrhenius behavior at moderate temperatures and show a rapid decrease or increase in rate constants above approximately 450 K. The reactions have different shapes of curves for the $\log_{10} k$ vs $1000/T$ plots, and the results indicate that our method is able to replicate all of these different
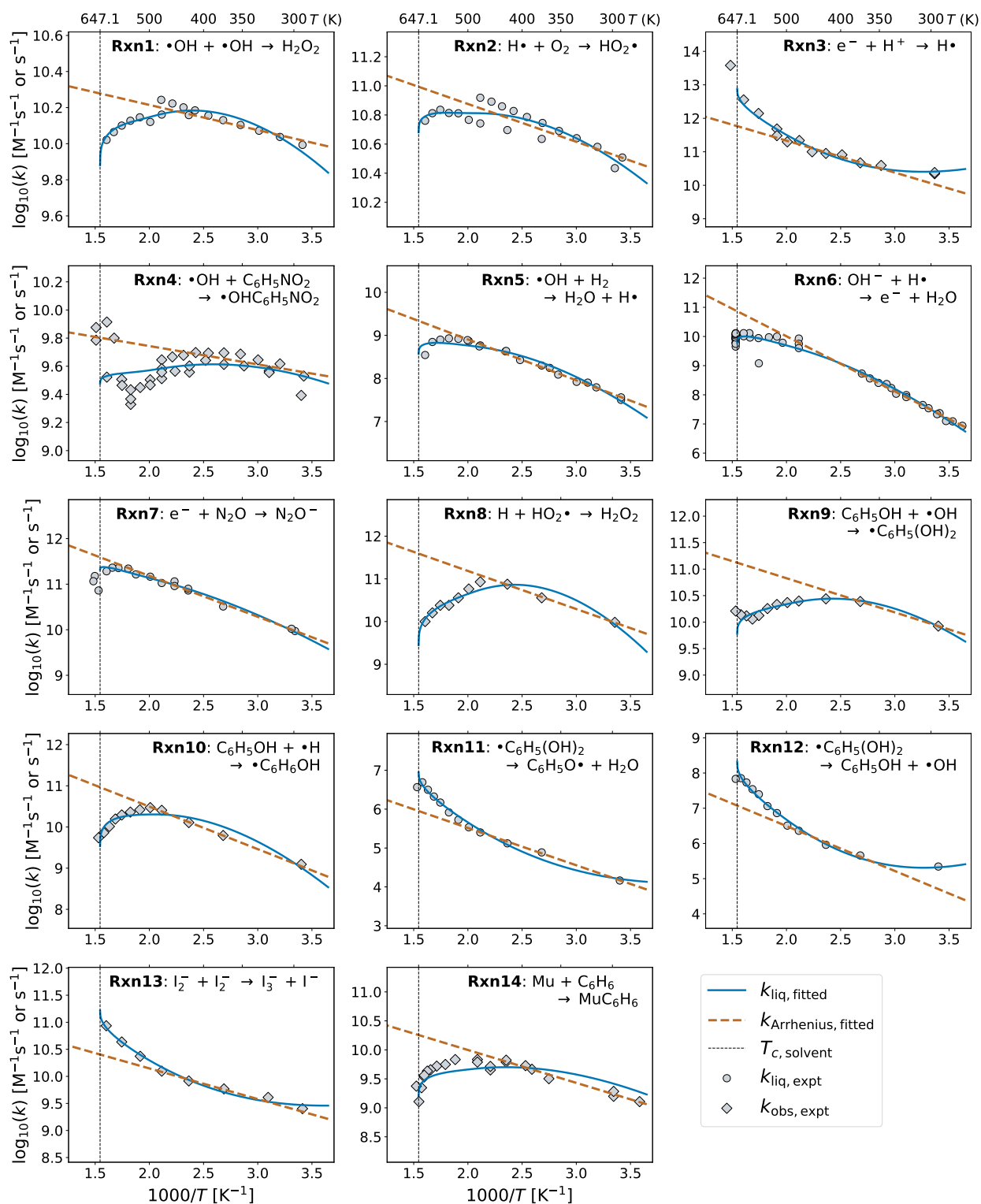
Figure 2: Comparison of the proposed functional form ($k_{\text{liq, fitted}}$, solid blue line) and the Arrhenius equation ($k_{\text{Arrhenius, fitted}}$, orange dashed line) fitted to the experimental rate constants. All reactions occur in water.

Table 2
Comparison of the overall $\log_{10} k_{\text{liq}}$ errors for each fitted functional form. Each reaction is weighted equally.

	Our functional form ($\log_{10} k_{\text{liq}}$ error)		Arrhenius eq ($\log_{10} k_{\text{liq}}$ error)	
T range considered	MAE	RMSE	MAE	RMSE
All T	0.07	0.09	0.25	0.35
$T \leq 400$ K	0.07	0.08	0.06	0.08
400 K $< T$	0.07	0.10	0.32	0.41

215 curvatures. The only exception is Reaction 4 for which our fitted function has a relatively higher error. Reaction 4 shows
216 an unusual trend where the rate constants start to decrease at around 460 K and then rapidly increase near the critical
217 temperature. Large deviations among the experimental data are also observed for Reaction 4 near the critical point as
218 there is one data point that has a much lower value compared to other data points at around the critical temperature.
219 Thus, it is possible that the relatively poor performance of our method on Reaction 4 is due to its high experimental
220 uncertainty.

221 The results also show that our method can accurately reproduce the observed rate constants of the reactions that are
222 influenced by diffusion limits. It is likely that the diffusion rate only affects the degree of the curvature of the $\log_{10} k$
223 vs $1000/T$ plot and does not dramatically change the general temperature dependence for the reaction. Since our
224 proposed functional form is able to fit to different shapes of curves, it is likely that it can also fit to the observed rate
225 constants of the diffusion-controlled reactions. To further validate our reasoning, we additionally fitted our functional
226 form to both $k_{\text{liq, expt}}$ and $k_{\text{obs, expt}}$ data for Reactions 1 and 2, which had both types of data available. The results
227 are presented in Figure 3. It can be seen that our method can correctly describe the temperature dependence of both
228 intrinsic and observed rate constants. As we expected, the two types of data differ only in the degree of curvature,
229 and their temperature trends are generally similar. Due to a lack of data, we are unable to perform the same analysis
230 for other reactions. Nonetheless, since our method shows good agreements with the experimental data for both the
231 reactions with and without diffusion effects as indicated by Figure 2, we anticipate the results to be similar for other
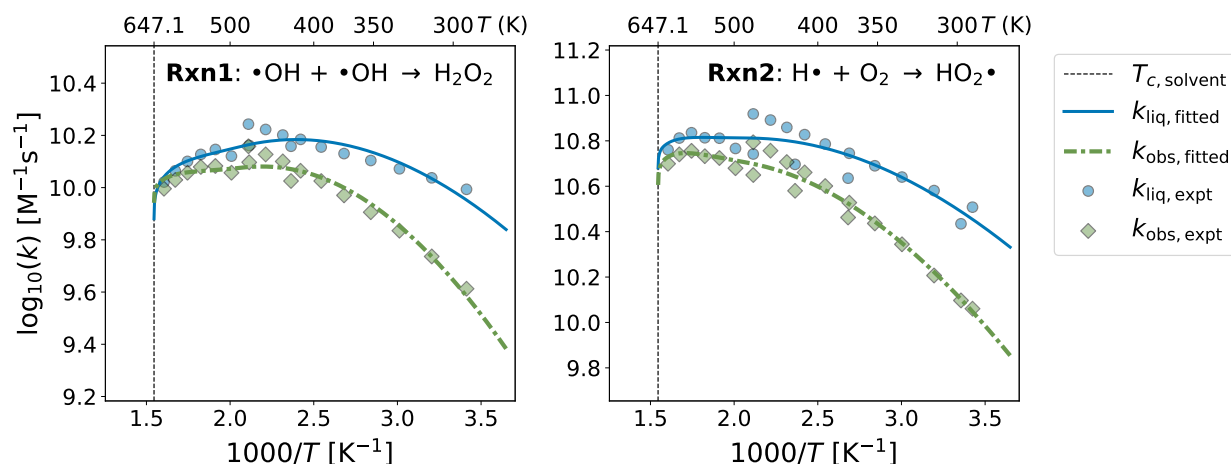232 reactions.

Figure 3: Comparison of the proposed functional forms fitted to the intrinsic liquid phase rate constants (k_{liq}, blue) and observed rate constants (k_{obs}, green).

233 The fitted empirical parameters of each reaction are provided in Table 3. The parameters have reasonable values for
234 all reactions as they were fitted using a constrained optimization method to obtain physically feasible solutions. The
235 magnitudes of the fitted A and E_a values are found to be similar between our functional form and the Arrhenius
236 equation. As mentioned earlier, our method assumes that the A and E_a terms are relevant to the gas phase contributions
237 while $\Delta\Delta G^{\ddagger}_{\text{solv}}(298$ K$)$ and $\Delta\Delta H^{\ddagger}_{\text{solv}}(298$ K$)$ account for the solvation effects. However, the optimized parameters

Table 3
Fitted kinetic parameters. E_a, $\Delta\Delta G^{\ddagger}_{\text{solv}}$(298 K), and $\Delta\Delta H^{\ddagger}_{\text{solv}}$(298 K) are in kcal/mol. A is in M^{-1}s^{-1} for a bimolecular reaction and in s^{-1} for a unimolecular reaction.

Rxn	Our functional form				Arrhenius eq	
	A	E_a	$\Delta\Delta G^{\ddagger}_{\text{solv}}$ (298 K)	$\Delta\Delta H^{\ddagger}_{\text{solv}}$ (298 K)	A	E_a
1	5.35e+10	2.51	-1.49	-0.62	3.12e+10	0.64
2	3.62e+11	2.60	-1.14	-0.37	2.48e+11	1.19
3	9.89e+13	3.30	1.59	-3.78	1.74e+13	4.36
4	6.78e+09	1.05	-0.66	-0.20	1.01e+10	0.60
5	4.16e+10	6.06	-1.89	0.71	6.31e+10	4.34
6	1.39e+13	9.94	-2.17	0.49	6.11e+13	8.64
7	1.16e+13	5.16	-0.90	0.15	9.50e+12	4.11
8	2.04e+11	5.51	-3.63	3.28	9.34e+12	4.08
9	6.46e+10	3.05	-1.89	1.48	1.31e+12	2.95
10	4.33e+12	9.18	-4.35	-1.21	3.65e+12	4.73
11	2.03e+08	4.03	1.54	-2.08	2.72e+07	4.39
12	5.77e+09	4.26	1.80	-4.83	1.12e+09	5.84
13	8.24e+11	2.07	1.25	-1.45	1.90e+11	2.59
14	3.96e+10	4.12	-2.51	-1.62	1.36e+11	2.60

are not guaranteed to correspond to the true values as they can have multiple solutions. Different initial guesses and constraints can yield different solutions, and it is difficult to determine which solution is closer to the true values. Our method also assumes that the gas phase rate constant follows the Arrhenius form, but some of the reactions are pressure-dependent in a gas phase and have non-Arrhenius behavior. Therefore, the fitted parameters should be treated as empirical parameters rather than the true kinetic parameters for the gas phase rate constants and solvation effects.

We additionally examined the contributions from the fitted gas phase parameters (A, E_a) and solvation parameters ($\Delta\Delta G^{\ddagger}_{\text{solv}}$(298 K), $\Delta\Delta H^{\ddagger}_{\text{solv}}$(298 K)) separately for our method. The results are provided for six representative reactions in Figure 4. The liquid phase rate constants estimated using all four parameters are presented in blue solid lines ($k_{\text{liq, fitted}}$), and the "gas phase" rate constants estimated using only A and E_a are presented in dotted red lines ($k_{\text{gas, fitted}}$). The gas phase kinetic parameters of Reactions 1, 2, and 5 could be found in literature, and therefore the gas phase rate constants are also computed using the literature values for these reactions and provided in the figure as black dash-dotted lines ($k_{\text{gas, literature}}$) for comparison. The literature values are obtained using RMG Database [61], which found multiple data for each reaction. The maximum and minimum rate constants estimated using different literature values are marked by the shaded area in the figure. Reactions 1 and 2 are identified as pressure-dependent, and their gas phase rate constants are computed at the saturation pressure of the solvent (sat. P) for all temperatures.

Figure 4 shows that the gas phase rate constants estimated using the fitted parameters deviate from the literature values for Reactions 1 and 2. This was expected as our method does not guarantee that the fitted parameters match the true values. Moreover, Reaction 1 has a non-linear temperature dependence in a gas phase that cannot be captured by the Arrhenius equation. On the contrary, the fitted gas phase rate constants show close agreement with the literature values for Reaction 5. Both Reactions 1 and 2 are pressure-dependent and assumed to be barrierless in a gas phase while Reaction 5 is independent of pressure and has a barrier height with a clearly defined transition state. It is hence possible that our approach can provide more accurate gas phase kinetic parameters for the reactions that have transition states and do not have pressure dependence. However, it is difficult to draw a solid conclusion as the comparison was made for only three reactions. More experimental data are needed for future studies to investigate whether the fitted parameters could yield reasonable estimates of gas phase rate constants. From Figure 4, it can be seen that the $k_{\text{gas,fitted}}$ values approach the $k_{\text{liq,fitted}}$ limits as temperature approaches the critical point. This is because our functional form forces the $\Delta\Delta G^{\ddagger}_{\text{solv}}(T)$ and k_{liq} to reach the limit of zero and k_{gas}, respectively, at the critical temperature. In fact, we can see that the literature gas phase rate constants of Reactions 1, 2, and 5 approach the same limit at around the critical point. The results seem to imply that our functional form approaches a correct limit. However, as mentioned
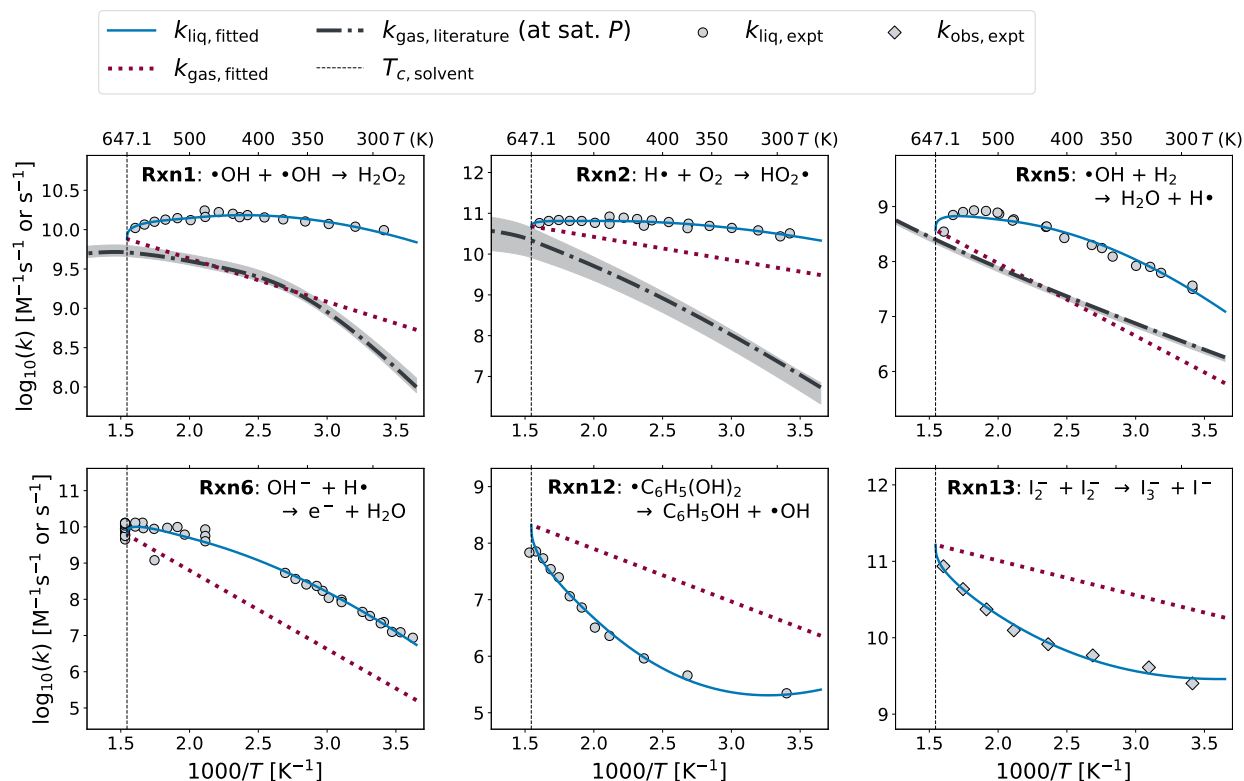
Figure 4: Comparison of the liquid phase rate constants estimated using all four parameters ($k_{\text{liq, fitted}}$, blue solid lines) and the gas phase rate constants estimated using only A and E_a ($k_{\text{gas, fitted}}$, red dotted line).

previously, the analysis was made only using three reactions, and more experimental data are required to further verify whether our approach can provide correct limits at the critical point.

4.2. Predicting the solvation parameters

New k_{liq} predictions are made based on the solvation parameters computed using the ab initio methods described in Section 2.3. In this approach, the solvation energies and enthalpies of reactants and TS are calculated at 298 K and combined together to get the $\Delta\Delta G^{\ddagger}_{\text{solv}}(298\ \text{K})$ and $\Delta\Delta H^{\ddagger}_{\text{solv}}(298\ \text{K})$ of a reaction. Then we applied our method to extrapolate $\Delta\Delta G^{\ddagger}_{\text{solv}}(T)$ from $\Delta\Delta G^{\ddagger}_{\text{solv}}(298\ \text{K})$ and $\Delta\Delta H^{\ddagger}_{\text{solv}}(298\ \text{K})$ and combined it with the literature k_{gas} data to make k_{liq} predictions. The solvation parameters, however, could be only calculated for the reaction that has a TS and has literature gas phase kinetic parameters. Only Reaction 5 matched this criteria, and thus the new predictions were made for only one reaction.

The results of the predicted k_{liq} are presented in Figure 5a along with the computed solvation parameters. We made additional predictions in Figure 5b by using the experimental solvation free energy and enthalpy data of the reactants that are obtained from various sources [62, 63, 64, 65, 66, 67]. Note that both figures use the same solvation energy and enthalpy values for the TS that are computed from the ab initio approach, and they only differ in the solvation values used for the reactants. The results show that Figure 5b provides more accurate predictions of k_{liq}. Figure 5a has a higher error at elevated temperatures, yet it also provides acceptable predictions overall. Both plots have similar $\Delta\Delta G^{\ddagger}_{\text{solv}}(298\ \text{K})$ values, but their $\Delta\Delta H^{\ddagger}_{\text{solv}}(298\ \text{K})$ values differ by around 2 kcal/mol. Our prior study [68] indicated that the COSMO-RS method, which is used to compute the solvation parameters, has a higher calculation error for solvation enthalpy compared to solvation free energy. Therefore, it is likely that the COSMO-RS method has relatively higher errors for the solvation enthalpies of the reactants, causing Figure 5a to underperform. Due to the paucity of the experimental data, the exact calculation errors of $\Delta\Delta G^{\ddagger}_{\text{solv}}(298\ \text{K})$ and $\Delta\Delta H^{\ddagger}_{\text{solv}}(298\ \text{K})$ and of k_{liq} cannot be determined for this approach.

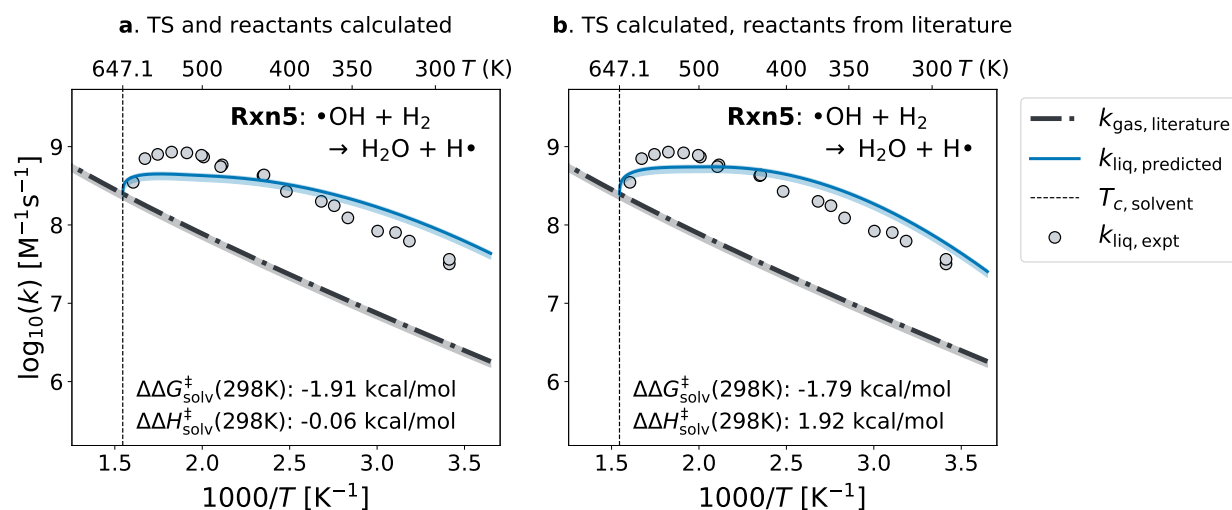**a**. TS and reactants calculated   **b**. TS calculated, reactants from literature

Figure 5: Result of the k_{liq} predictions from the calculated solvation kinetic parameters. (a) The ΔG_{solv}(298 K) and ΔH_{solv}(298 K) of both TS and reactants are calculated using ab initio methods. (b) Only the ΔG_{solv}(298 K) and ΔH_{solv}(298 K) of the TS is calulcated using ab intio method, and those of the reactants are obtained from literature.

Overall, it is found that our method can achieve reliable predictions of temperature-dependent liquid phase rate constants for Reaction 5 based on the computed or experimental solvation parameters. This suggests that our proposed expression can serve not only as an empirical functional form but also as a predictive method. Nonetheless, the analysis was limited to only one reaction, and more thorough assessments should be made with more experimental data to determine whether our method can also provide accurate predictions for different reactions.

5. Conclusions

We have developed a new functional form that can describe the temperature dependence of liquid phase rate constants for various reactions. The proposed method employs four kinetic parameters, two associated with the gas phase contributions and other two associated with the solvation corrections. These parameters can be fitted to experimental liquid phase rate constants to accurately reproduce the experimental data from room temperature up to the critical temperature of a solvent. The method was evaluated using 14 reactions, and the results reveal that our method showed superior performance at elevated temperatures compared to the Arrhenius equation. The four kinetic parameters have physical meanings and can be also calculated using ab initio methods instead of empirically fitting to the data. A preliminary result implies that the solvation parameters can be computed using the quantum chemistry and COSMO-RS methods to make the k_{liq} predictions. Moving forward, future studies should look to collect more experimental data to further evaluate our proposed method and to test whether the kinetic parameters can be accurately calculated using ab initio approaches.

CRediT authorship contribution statement

Yunsie Chung: Conceptualization, Methodology, Data Curation, Validation, Visualization, Writing - Original Draft.
William H. Green: Supervision, Funding acquisition, Resources, Writing - Review & Editing.

Declaration of competing interest

The authors declare that they have no known competing financial interests or personal relationships that could have appeared to influence the work reported in this paper.

Data availability

The experimental data collected from literature for method validation are provided as Supplementary data.

Acknowledgements

References

[1] J. T. Reaves, C. B. Roberts, Subcritical solvent effects on a parallel Diels-Alder reaction network, Ind. Eng. Chem. Res. 38 (3) (1999) 855–864. https://doi.org/10.1021/ie980474v.

[2] P. Krammer, H. Vogel, Hydrolysis of esters in subcritical and supercritical water, J. Supercrit. Fluids 16 (3) (2000) 189–206. https://doi.org/10.1016/S0896-8446(99)00032-7.

[3] Ž. Knez, M. Leitgeb, M. Primožič, Chemical Reactions in Subcritical and Supercritical Fluids, in: R.A. Meyers (Ed.), Encyclopedia of Sustainability Science and Technology, Springer New York, New York, NY, 2018, pp. 1–21.

[4] Ž. Knez, M. Pantić, D. Cör, Z. Novak, M. Knez Hrnčič, Are supercritical fluids solvents for the future?, Chem. Eng. Process.- Process Intensif. 141 (2019) 107532. https://doi.org/10.1016/j.cep.2019.107532.

[5] M. Watanabe, T. Sato, H. Inomata, R. L. Smith, K. Arai, A. Kruse, E. Dinjus, Chemical reactions of C1 compounds in near-critical and supercritical water, Chem. Rev. 104 (12) (2004) 5803–5821. https://doi.org/10.1021/cr020415y.

[6] A. A. Galkin, V. V. Lunin, Subcritical and supercritical water: A universal medium for chemical reactions, Russ. Chem. Rev. 74 (1) (2005) 21. https://doi.org/10.1070/rc2005v074n01abeh001167.

[7] N. Simsek Kus, Organic reactions in subcritical and supercritical water, Tetrahedron 68 (4) (2012) 949–958. https://doi.org/10.1016/j.tet.2011.10.070.

[8] Y. Park, J. T. Reaves, C. W. Curtis, C. B. Roberts, Conversion of Tire Waste Using Subcritical and Supercritical Water Oxidation, J. Elastomers Plast. 31 (2) (1999) 162–179. https://doi.org/10.1177/009524439903100205.

[9] R. Morales Ibarra, M. Sasaki, M. Goto, A. T. Quitain, S. M. García Montes, J. A. Aguilar-Garib, Carbon fiber recovery using water and benzyl alcohol in subcritical and supercritical conditions for chemical recycling of thermoset composite materials, J. Mater. Cycles Waste Manag. 17 (2015) 369–379. https://doi.org/10.1007/s10163-014-0252-z.

[10] M. Goto, Subcritical and supercritical fluid technology for recycling waste plastics, J. Jpn. Pet. Inst. 59 (6) (2016) 254–258. https://doi.org/10.1627/jpi.59.254.

[11] I. Okajima, K. Watanabe, S. Haramiishi, M. Nakamura, Y. Shimamura, T. Sako, Recycling of carbon fiber reinforced plastic containing amine-cured epoxy resin using supercritical and subcritical fluids, J. Supercrit. Fluids 119 (2017) 44–51. https://doi.org/10.1016/j.supflu.2016.08.015.

[12] M. Möller, P. Nilges, F. Harnisch, U. Schröder, Subcritical water as reaction environment: Fundamentals of hydrothermal biomass transformation, ChemSusChem 4 (5) (2011) 566–579. https://doi.org/10.1002/cssc.201000341.

[13] N. Galy, R. Nguyen, H. Yalgin, N. Thiebault, D. Luart, C. Len, Glycerol in subcritical and supercritical solvents, J. Chem. Technol. Biotechnol. 92 (1) (2017) 14–26. https://doi.org/10.1002/jctb.5101.

[14] A. Yüksel Özşen, Conversion of Biomass to Organic Acids by Liquefaction Reactions Under Subcritical Conditions, Front. Chem. 8 (2020) 24. https://doi.org/10.3389/fchem.2020.00024.

[15] A. J. Elliot, D. R. McCracken, G. V. Buxton, N. D. Wood, Estimation of rate constants for near-diffusion-controlled reactions in water at high temperatures, J. Chem. Soc., Faraday Trans. 86 (1990) 1539–1547. https://doi.org/10.1039/ft9908601539.

[16] T. W. Marin, C. D. Jonah, D. M. Bartels, Reaction of OH* radicals with H_2 in sub-critical water, Chem. Phys. Lett. 371 (1) (2003) 144–149. https://doi.org/10.1016/S0009-2614(03)00064-2.

[17] K. Ghandi, B. Addison-Jones, J. Brodovitch, S. Kecman, I. McKenzie, P. Percival, Muonium kinetics in sub- and supercritical water, Phys. B: Condens. Matter. 326 (1-4) (2003) 55–60. https://doi.org/10.1016/S0921-4526(02)01572-7.

[18] G. Liu, C. Landry, K. Ghandi, Prediction of rate constants of important chemical reactions in water radiation chemistry in sub and supercritical water-non-equilibrium reactions, Can. J. Chem. 96 (2) (2018) 267–279. https://doi.org/10.1139/cjc-2017-0315.

[19] S. Arrhenius, Über die Reaktionsgeschwindigkeit bei der Inversion von Rohrzucker durch Säuren, Zeitschrift für Physikalische Chemie 4U (1) (1889) 226–248. https://doi.org/10.1515/zpch-1889-0416.

[20] J. Bonin, I. Janik, D. Janik, D. M. Bartels, Reaction of the hydroxyl radical with phenol in water up to supercritical conditions, J. Phys. Chem. A 111 (10) (2007) 1869–1878. https://doi.org/10.1021/jp0665325.

[21] I. Janik, D. M. Bartels, T. W. Marin, C. D. Jonah, Reaction of O_2 with the hydrogen atom in water up to 350 °C, J. Phys. Chem. A 111 (1) (2007) 79–88. https://doi.org/10.1021/jp065140v.

[22] Y. Muroya, S. Yamashita, P. Lertnaisat, S. Sanguanmith, J. Meesungnoen, J. P. Jay-Gerin, Y. Katsumura, Rate constant for the $H^\cdot + H_2O \longrightarrow {}^\cdot OH + H_2$ reaction at elevated temperatures measured by pulse radiolysis, Phys. Chem. Chem. Phys. 19 (2017) 30834–30841. https://doi.org/10.1039/c7cp06010f.

[23] P. A. Marrone, T. A. Arias, W. A. Peters, J. W. Tester, Solvation Effects on Kinetics of Methylene Chloride Reactions in Sub- and Supercritical Water: Theory, Experiment, and Ab Initio Calculations, J. Phys. Chem. A 102 (35) (1998) 7013–7028. https://doi.org/10.1021/jp981257a.

[24] D. Salvatierra, J. D. Taylor, P. A. Marrone, J. W. Tester, Kinetic Study of Hydrolysis of Methylene Chloride from 100 to 500 °C, Ind. Eng. Chem. Res. 38 (11) (1999) 4169–4174. https://doi.org/10.1021/ie9903700.

[25] N. Akiya, P. E. Savage, Roles of Water for Chemical Reactions in High-Temperature Water, Chem. Rev. 102 (8) (2002) 2725–2750. https://doi.org/10.1021/cr000668w.

[26] A. Jalan, R. H. West, W. H. Green, An extensible framework for capturing solvent effects in computer generated kinetic models, J. Phys. Chem. B 117 (10) (2013) 2955–2970. https://doi.org/10.1021/jp310824h.

[27] J. G. Kirkwood, Theory of Solutions of Molecules Containing Widely Separated Charges with Special Application to Zwitterions, J. Chem. Phys. 2 (7) (1934) 351–361. https://doi.org/10.1063/1.1749489.

[28] Y. Chung, R. J. Gillis, W. H. Green, Temperature-dependent vapor–liquid equilibria and solvation free energy estimation from minimal data, AIChE J. 66 (6) (2020) e16976. https://doi.org/https://doi.org/10.1002/aic.16976.

[29] A. Harvey, Semiempirical correlation for Henry's constants over large temperature ranges, AlChE J. 42 (5) (1996) 1491–1494. https://doi.org/10.1002/aic.690420531.

[30] M. L. Japas, J. M. H. L. Sengers, Gas solubility and Henry's law near the solvent's critical point, AlChE J. 35 (5) (1989) 705–713. https://doi.org/10.1002/aic.690350502.

[31] Y. Chung, W. H. Green, Computing Kinetic Solvent Effects and Liquid Phase Rate Constants Using Quantum Chemistry and COSMO-RS Methods, J. Phys. Chem. A 127 (27) (2023) 5637–5651. https://doi.org/10.1021/acs.jpca.3c01825.

[32] Y. Chung, W. H. Green, Machine learning from quantum chemistry to predict experimental solvent effects on reaction rates, Chem. Sci. 15 (7) (2024) 2410–2424. https://doi.org/10.1039/D3SC05353A.

[33] I. H. Bell, J. Wronski, S. Quoilin, V. Lemort, Pure and pseudo-pure fluid thermophysical property evaluation and the open-source thermophysical property library coolprop, Ind. Eng. Chem. Res. 53 (6) (2014) 2498–2508. https://doi.org/10.1021/ie4033999.

[34] P. J. Walker, H.-W. Yew, A. Riedemann, Clapeyron.jl: An Extensible, Open-Source Fluid Thermodynamics Toolkit, Ind. Eng. Chem. Res. 61 (20) (2022) 7130–7153. https://doi.org/10.1021/acs.iecr.2c00326.

[35] S. Biswas, Y. Chung, J. Ramirez, H. Wu, W. H. Green, Predicting Critical Properties and Acentric Factors of Fluids Using Multitask Machine Learning, J. Chem. Inf. Model. 63 (15) (2023) 4574–4588. https://doi.org/10.1021/acs.jcim.3c00546.

[36] P. Virtanen, R. Gommers, T. E. Oliphant, M. Haberland, T. Reddy, D. Cournapeau, E. Burovski, P. Peterson, W. Weckesser, J. Bright, S. J. van der Walt, M. Brett, J. Wilson, K. J. Millman, N. Mayorov, A. R. J. Nelson, E. Jones, R. Kern, E. Larson, C. J. Carey, I. Polat, Y. Feng, E. W. Moore, J. VanderPlas, D. Laxalde, J. Perktold, R. Cimrman, I. Henriksen, E. A. Quintero, C. R. Harris, A. M. Archibald, A. H. Ribeiro, F. Pedregosa, P. van Mulbregt, SciPy 1.0 Contributors, SciPy 1.0: Fundamental Algorithms for Scientific Computing in Python, Nat. Methods 17 (2020) 261–272. https://doi.org/10.1038/s41592-019-0686-2.

[37] J. D. Chai, M. Head-Gordon, Long-range corrected hybrid density functionals with damped atom-atom dispersion corrections, Phys. Chem. Chem. Phys. 10 (44) (2008) 6615–6620. https://doi.org/10.1039/b810189b.

[38] F. Weigend, Accurate Coulomb-fitting basis sets for H to Rn, Phys. Chem. Chem. Phys. 8 (9) (2006) 1057–1065. https://doi.org/10.1039/b515623h.

[39] M. J. Frisch, G. W. Trucks, H. B. Schlegel, G. E. Scuseria, M. A. Robb, J. R. Cheeseman, G. Scalmani, V. Barone, G. A. Petersson, H. Nakatsuji, X. Li, M. Caricato, A. V. Marenich, J. Bloino, B. G. Janesko, R. Gomperts, B. Mennucci, H. P. Hratchian, J. V. Ortiz, A. F. Izmaylov, J. L. Sonnenberg, D. Williams-Young, F. Ding, F. Lipparini, F. Egidi, J. Goings, B. Peng, A. Petrone, T. Henderson, D. Ranasinghe, V. G. Zakrzewski, J. Gao, N. Rega, G. Zheng, W. Liang, M. Hada, M. Ehara, K. Toyota, R. Fukuda, J. Hasegawa, M. Ishida, T. Nakajima, Y. Honda, O. Kitao, H. Nakai, T. Vreven, K. Throssell, J. A. Montgomery Jr., J. E. Peralta, F. Ogliaro, M. J. Bearpark, J. J. Heyd, E. N. Brothers, K. N. Kudin, V. N. Staroverov, T. A. Keith, R. Kobayashi, J. Normand, K. Raghavachari, A. P. Rendell, J. C. Burant, S. S. Iyengar, J. Tomasi, M. Cossi, J. M. Millam, M. Klene, C. Adamo, R. Cammi, J. W. Ochterski, R. L. Martin, K. Morokuma, O. Farkas, J. B. Foresman, D. J. Fox, Gaussian 16 Revision C.01, Gaussian Inc. Wallingford CT (2016).

[40] A. Klamt, Conductor-like Screening Model for Real Solvents: A New Approach to the Quantitative Calculation of Solvation Phenomena, J. Phys. Chem. 99 (7) (1995) 2224–2235. https://doi.org/10.1021/j100007a062. https://pubs.acs.org/doi/10.1021/j100007a062

[41] A. Klamt, V. Jonas, T. Bürger, J. C. W. Lohrenz, Refinement and Parametrization of COSMO-RS, J. Phys. Chem. A 102 (26) (1998) 5074–5085. https://doi.org/10.1021/jp980017s.

[42] F. Eckert, A. Klamt, Fast solvent screening via quantum chemistry: COSMO-RS approach, AlChE J. 48 (2) (2002) 369–385. https://doi.org/10.1002/aic.690480220.

[43] J. P. Perdew, Density-functional approximation for the correlation energy of the inhomogeneous electron gas, Phys. Rev. B 33 (12) (1986) 8822–8824. https://doi.org/10.1103/PhysRevB.33.8822.

[44] A. D. Becke, Density-functional exchange-energy approximation with correct asymptotic behavior, Phys. Rev. A 38 (6) (1988) 3098–3100. https://doi.org/10.1103/PhysRevA.38.3098.

[45] D. Rappoport, F. Furche, Property-optimized Gaussian basis sets for molecular response calculations, J. Chem. Phys. 133 (13) (2010) 134105. https://doi.org/10.1063/1.3484283.

[46] A. Klamt, M. Diedenhofen, A refined cavity construction algorithm for the conductor-like screening model, J. Comput. Chem. 39 (21) (2018) 1648–1655. https://doi.org/10.1002/jcc.25342.

[47] *TURBOMOLE*, version 7.5; a development of University of Karlsruhe and Forschungszentrum Karlsruhe GmbH; TURBOMOLE GmbH: Karlsruhe, Germany, 2020. https://www.turbomole.org (accessed 17 March 2024).

[48] S. G. Balasubramani, G. P. Chen, S. Coriani, M. Diedenhofen, M. S. Frank, Y. J. Franzke, F. Furche, R. Grotjahn, M. E. Harding, C. Hättig, A. Hellweg, B. Helmich-Paris, C. Holzer, U. Huniar, M. Kaupp, A. Marefat Khah, S. Karbalaei Khani, T. Müller, F. Mack, B. D. Nguyen, S. M. Parker, E. Perlt, D. Rappoport, K. Reiter, S. Roy, M. Rückert, G. Schmitz, M. Sierka, E. Tapavicza, D. P. Tew, C. van Wüllen, V. K. Voora, F. Weigend, A. Wodyński, J. M. Yu, TURBOMOLE: Modular program suite for ab initio quantum-chemical and condensed-matter simulations, J. Chem. Phys. 152 (18) (2020) 184107. https://doi.org/10.1063/5.0004635.

[49] Dassault Systèmes, BIOVIA COSMOtherm, Release 2020. http://www.3ds.com, 2020 (accessed 17 March 2024).

[50] I. Janik, D. M. Bartels, C. D. Jonah, Hydroxyl radical self-recombination reaction and absorption spectrum in water up to 350°C, J. Phys. Chem. A 111 (10) (2007) 1835–1843. https://doi.org/10.1021/jp065992v.

[51] G. Wu, Y. Katsumura, M. Lin, T. Morioka, Y. Muroya, Temperature dependence of ketyl radical in aqueous benzophenone solutions up to 400°C: A pulse radiolysis study, Phys. Chem. Chem. Phys. 4 (16) (2002) 3980–3988. https://doi.org/10.1039/b203914c.

[52] H. Shiraishi, G. R. Sunaryo, K. Ishigure, Temperature Dependence of Equilibrium and Rate Constants of Reactions Inducing Conversion between Hydrated Electron and Atomic Hydrogen, J. Phys. Chem. 98 (19) (1994) 5164–5173. https://doi.org/10.1021/j100070a037.

[53] K. Ghandi, P. W. Percival, Prediction of rate constants for reactions of the hydroxyl radical in water at high temperatures and pressures, J. Phys. Chem. A 107 (17) (2003) 3005–3008. https://doi.org/10.1021/jp027858q.

[54] L. Ashton, G. V. Buxton, C. R. Stuart, Temperature dependence of the rate of reaction of OH with some aromatic compounds in aqueous solution. Evidence for the formation of a π-complex intermediate?, J. Chem. Soc., Faraday Trans. 91 (11) (1995) 1631–1633. https://doi.org/10.1039/FT9959101631.

[55] J. Feng, S. N. V. K. Aki, J. E. Chateauneuf, J. F. Brennecke, Hydroxyl Radical Reactivity with Nitrobenzene in Subcritical and Supercritical Water, J. Am. Chem. Soc. 124 (22) (2002) 6304–6311. https://doi.org/10.1021/ja0110980.

[56] T. W. Marin, J. A. Cline, K. Takahashi, D. M. Bartels, C. D. Jonah, Pulse Radiolysis of Supercritical Water. 2. Reaction of Nitrobenzene with Hydrated Electrons and Hydroxyl Radicals, J. Phys. Chem. A 106 (51) (2002) 12270–12279. https://doi.org/10.1021/jp026812u.

[57] H. Christensen, K. Sehested, Reaction of hydroxyl radicals with hydrogen at elevated temperatures. Determination of the activation energy, J. Phys. Chem. 87 (1) (1983) 118–120. https://doi.org/10.1021/j100224a027.

[58] J. Cline, K. Takahashi, T. W. Marin, C. D. Johan, D. M. Bartels, Pulse radiolysis of supercritical water. 1. Reactions between hydrophobic and anionic species, J. Phys. Chem. A 106 (51) (2002) 12260–12269. https://doi.org/10.1021/jp0270250.

[59] P. Han, D. M. Bartels, Hydrogen/deuterium isotope effects in water radiolysis. 4. The mechanism of $(H)_{aq} \rightleftharpoons (e^-)_{aq}$ interconversion, J. Phys. Chem. 96 (12) (1992) 4899–4906. https://doi.org/10.1021/j100191a033.

[60] K. Takahashi, S. Ohgami, Y. Koyama, S. Sawamura, T. W. Marin, D. M. Bartels, C. D. Jonah, Reaction rates of the hydrated electron with N_2O in high temperature water and potential surface of the N_2O^- anion, Chem. Phys. Lett. 383 (5-6) (2004) 445–450. https://doi.org/10.1016/j.cplett.2003.11.050.

[61] M. S. Johnson, X. Dong, A. Grinberg Dana, Y. Chung, D. Farina, R. J. Gillis, M. Liu, N. W. Yee, K. Blondal, E. Mazeau, C. A. Grambow, A. M. Payne, K. A. Spiekermann, H.-W. Pang, C. F. Goldsmith, R. H. West, W. H. Green, RMG Database for Chemical Property Prediction, J. Chem. Inf. Model. 62 (20) (2022) 4906–4915. https://doi.org/10.1021/acs.jcim.2c00965.

[62] D. R. Hanson, J. B. Burkholder, C. J. Howard, A. R. Ravishankara, Measurement of hydroxyl and hydroperoxy radical uptake coefficients on water and sulfuric acid surfaces, J. Phys. Chem. 96 (12) (1992) 4979–4985. https://doi.org/10.1021/j100191a046.

[63] R. Sander, Compilation of Henry's law constants (version 4.0) for water as solvent, Atmospheric Chemistry and Physics 15 (8) (2015) 4399–4981. https://doi.org/10.5194/acp-15-4399-2015.

[64] T. Autrey, A. K. Brown, D. M. Camaioni, M. Dupuis, N. S. Foster, A. Getty, Thermochemistry of Aqueous Hydroxyl Radical from Advances in Photoacoustic Calorimetry and ab Initio Continuum Solvation Theory, J. Am. Chem. Soc. 126 (12) (2004) 3680–3681. https://doi.org/10.1021/ja039827u.

[65] P. Cabral do Couto, R. C. Guedes, B. J. Costa Cabral, J. A. Martinho Simões, The hydration of the OH radical: Microsolvation modeling and statistical mechanics simulation, J. Chem. Phys. 119 (14) (2003) 7344–7355. https://doi.org/10.1063/1.1605939.

[66] A. S. McNeill, C.-G. Zhan, A. M. Appel, D. M. Stanbury, D. A. Dixon, The H•/H⁻ Redox Couple and Absolute Hydration Energy of H⁻, J. Phys. Chem. A 124 (29) (2020) 6084–6095. https://doi.org/10.1021/acs.jpca.0c03833.

[67] M. Szeląg, A. Urbaniak, H. A. Bluyssen, A theoretical antioxidant pharmacophore for natural hydroxycinnamic acids, Open Chem. 13 (1) (2015) 000010151520150001. https://doi.org/10.1515/chem-2015-0001.

[68] Y. Chung, F. H. Vermeire, H. Wu, P. J. Walker, M. H. Abraham, W. H. Green, Group Contribution and Machine Learning Approaches to Predict Abraham Solute Parameters, Solvation Free Energy, and Solvation Enthalpy, J. Chem. Inf. Model. 62 (3) (2022) 433–446. https://doi.org/10.1021/acs.jcim.1c01103.